Supporting Information for The Stability Transition from Stable to Unstable Frictional Slip with Finite Pore Pressure

R. Affinito[1], C. Wood[1], S. Marty[1], D. Elsworth[1,3], C. Marone[1,2]

[1]Department of Geoscience, Pennsylvania State University

[2]Dipartimento di Scienze della Terra, La Sapienza Università di Roma

[3]Deptartment of Energy and Mineral Engineering, EMS Energy Institute, and G3 Center, Pennsylvania State University

[1]Department of Geosciences, 503 Deike Building, University Park, PA 16802 USA

[2]EMS Energy Institute, Penn State University, C-211 Coal Utilization Laboratory, University Park, PA 16802 USA

[3]Department of Earth Sciences, La Sapienza University of Rome, P.le Aldo Moro, 5 - 00185 Rome, Italy

Corresponding author: R. A. Affinito, Department of Geosciences, 503 Deike Building, University Park, PA 16802 USA (affinito@psu.edu)

March 14, 2023, 9:05pm

Additional Supporting Information (Files uploaded separately)

1. Supporting datasets uploaded to the following:

Contents of this file

1. Table 1: Experimental List

2. Supplement 1: Experiment Overview

3. Supplement 2: Stick Slip Picking Method

4. Supplement 3: Stiffness Measurement Method

5. Supplement 4: Confining Pressure Stiffness Calibration

6. Supplement 5: Fault Loading Creep Velocity

7. Supplement 6: Permeability Evolution

8. Supplement 7: Fault Dilation and Fluid Volume Flux

9. Supplement 8 Stress Drop Statistics For All Experiments

March 14, 2023, 9:05pm

Introduction

22   The following information was collected alongside the data presented in the manuscript.

23   Reported below is an overview of the experiments conducted, calibrations, and measure-

24   ments that support the recorded findings. No known anomalies are recorded within the

25   data. Any and all information can be provided upon request.

26

27 **Supplemental Table**

| ID	σ_n [MPa]	P_p [MPa]	P_c [MPa]	λ	Loading Velocity [$\frac{\mu m}{s}$]	Slip Type
P5609	15	0	0	0	1,3,10	Stable
P5610	17	5	10	0.2	10	Unstable
P5611	18	5	8	0.25	10	Unstable
P5612	20	4	5	0.22	1,3,10	Stable
P5613	15	5	10	0.2	10	Unstable
p5633	18	1	5	0.05	10	Unstable
P5637	19	2	5	0.09	10	Unstable
P5638	19	2	5	0.09	10	Unstable
P5640	20	3	5	0.12	10	Unstable
P5661	21	4	5	0.2	10	Unstable
P5705	21	4	5	0.2	10	Unstable
P5722	21	4	5	0.2	10	Unstable
P5723	20	3	5	0.12	10	Unstable
P5724	19	2	5	0.09	10	Unstable
P5725	18	1	5	0.05	10	Unstable
P5804	21	4	5	0.2	3, 10, 30	Stable

Table S1.   Experiment List

March 14, 2023, 9:05pm
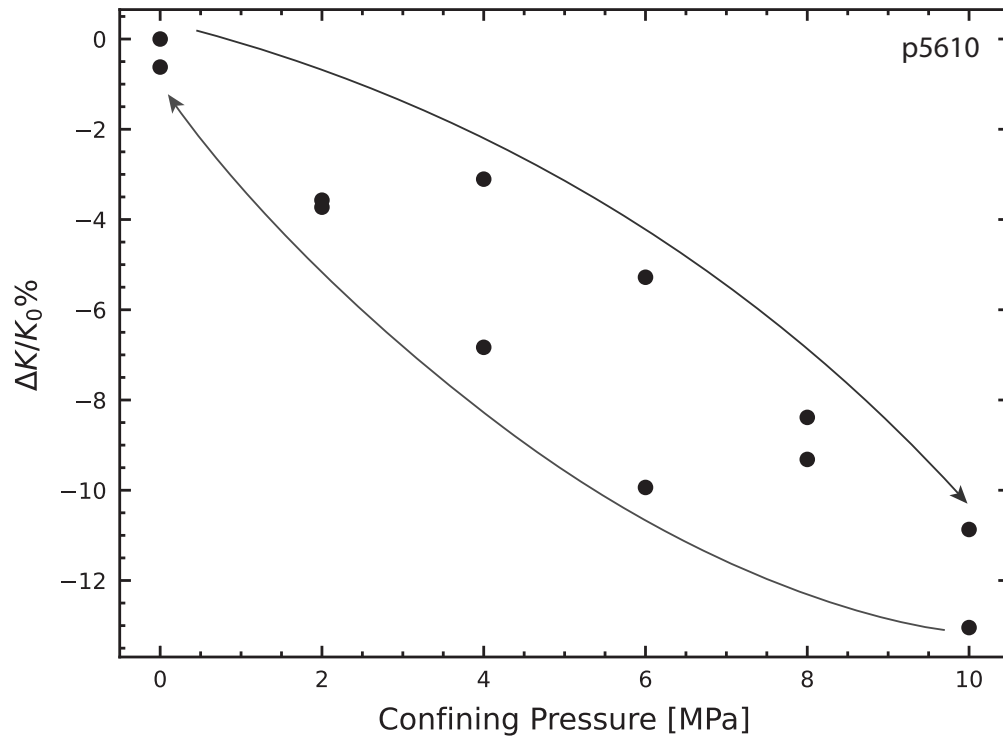
Figure S1. Measurements of the loading stiffness made from shear load/unload cycles at confining pressures from 0 to 10 MPa. These are effective stiffness values and include the acrylic spring inside the pressure vessel, the load frame and the fault zones. Note that the changes are roughly 1% per 1MPa of confining pressure. Experiments were done at 5 MPa confining pressure.

March 14, 2023, 9:05pm
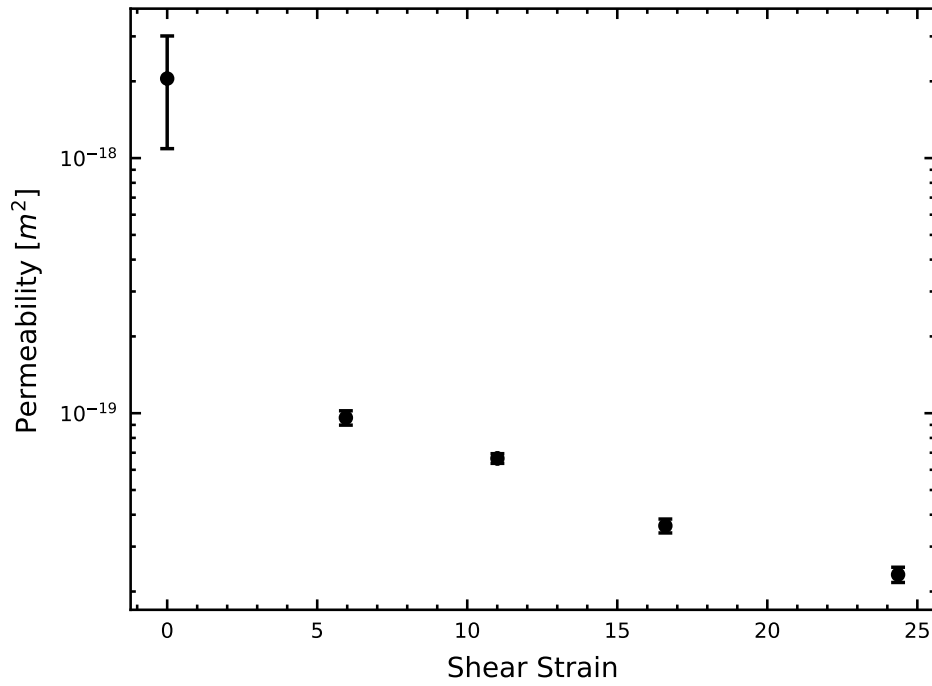
Figure S2.   Permeability normal to the fault zones as a function of shear strain. The changes are largest during initial shear, for shear strains up to 10, when the fault zones are compacting. Error bars show the degree of variability from repeat measurements.
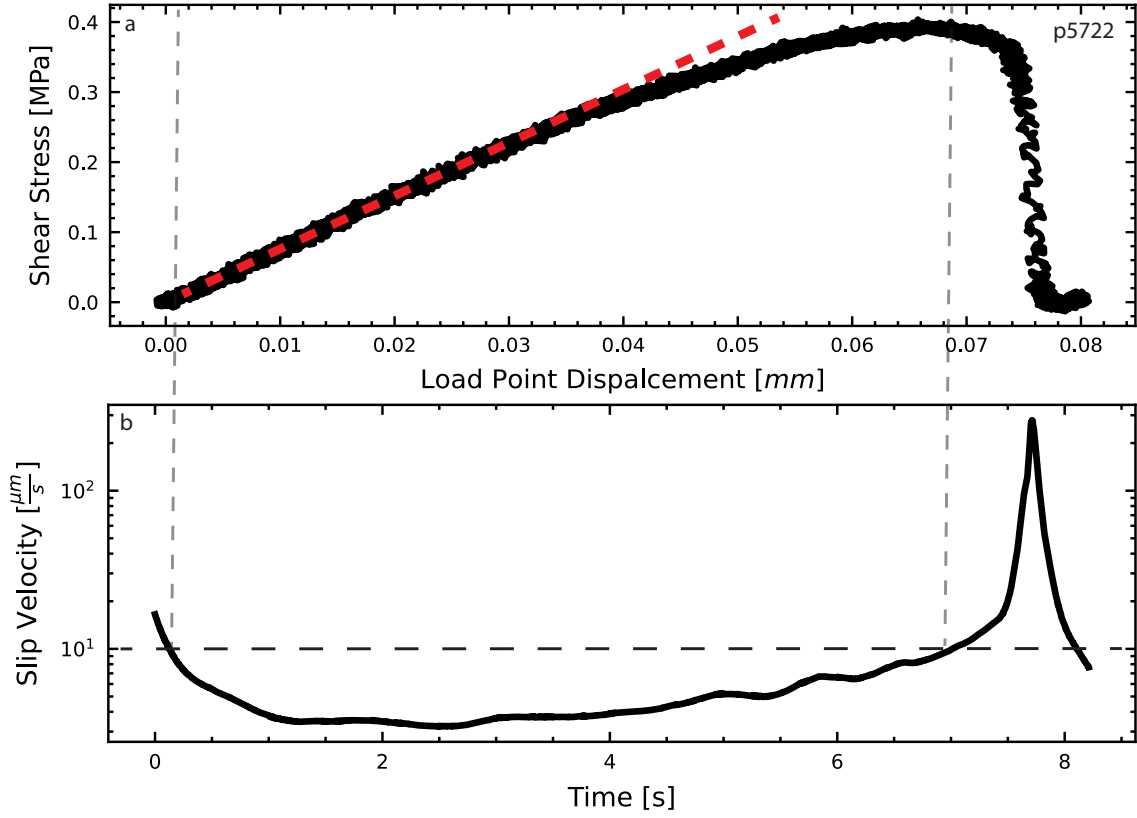
Figure S3.   Example of the stiffness measurement technique. Part of a lab seismic cycle is shown as shear stress versus load point displacement (a), and the corresponding fault slip velocity (b). The data window is chosen by where the event 'locks' (green dot - slip velocity drops below the background loading rate) and it extends to the unlocking stage (red dot - slip velocity surpasses the background loading rate). A linear fit is done from the green dot, until the standard deviation increases past a threshold (a). As such, the linear fit is weighted toward the section with the lowest fault creep velocity (b)

March 14, 2023, 9:05pm
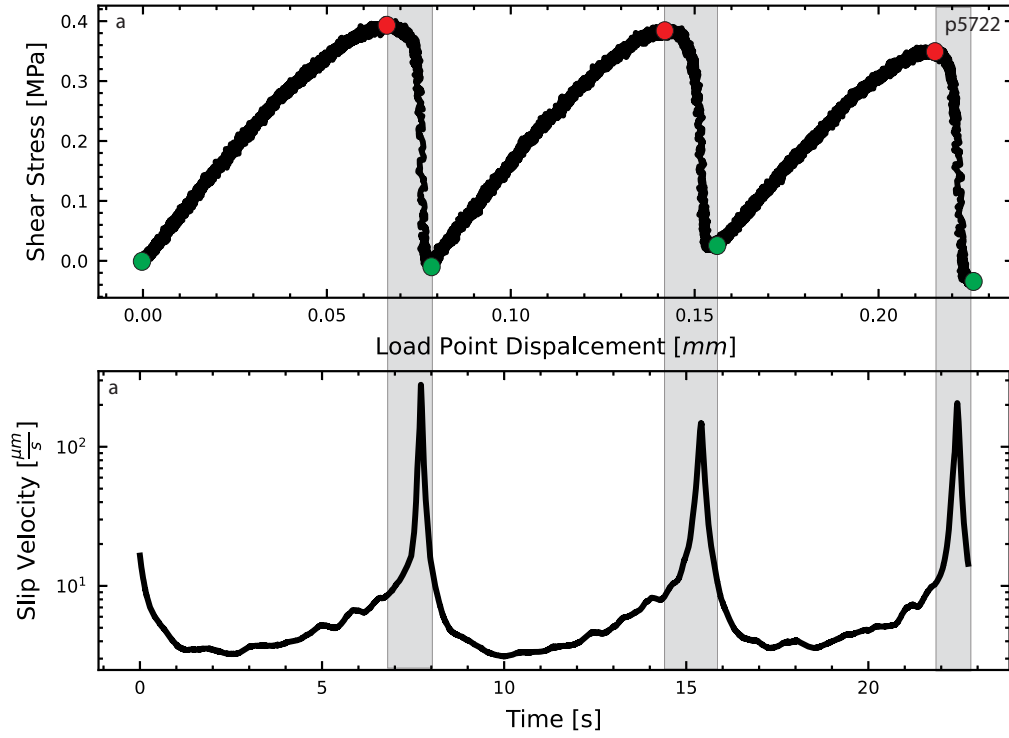
Figure S4. Example of stick-slip picking method. Three laboratory stick-slip cycles in shear stress as a function of load point displacement (a) and slip velocity as a function of time (b). For each event, the maximum shear stress (red dot), and the following minimum (green dot) are indexed. The maximum and minimum are used to define the co- and interseismic periods (co-seismic stages are outlined in grey). All experiments are indexed with the same method for consistency.
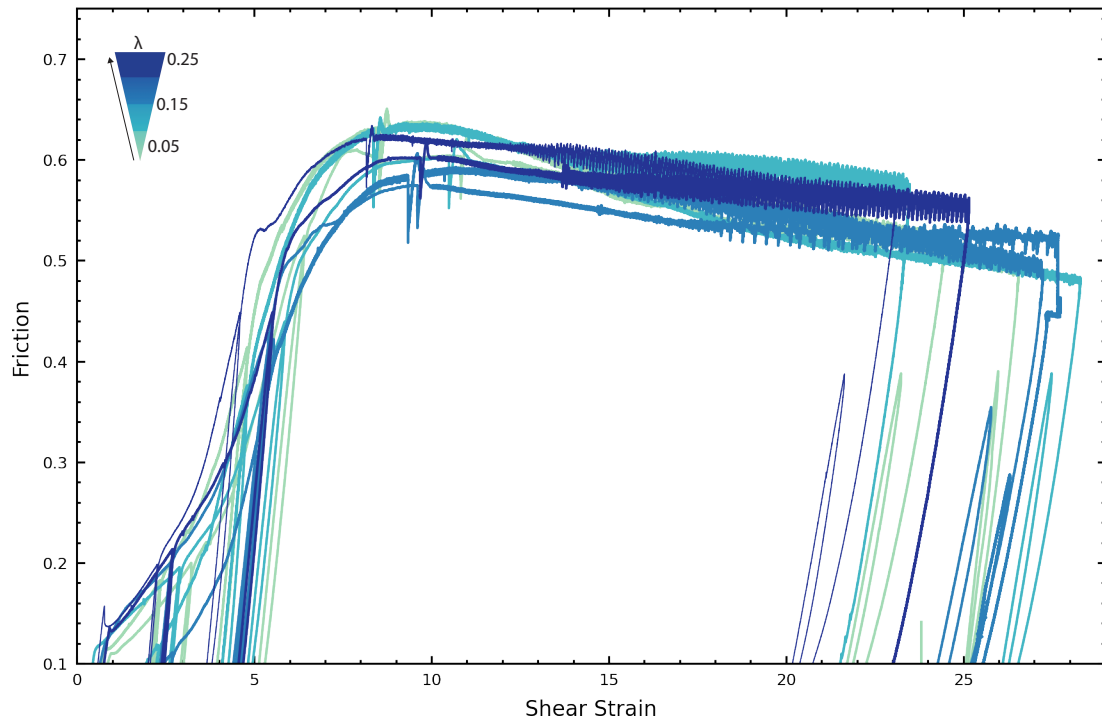
Figure S5. Friction versus shear strain plots for all stick-slip experiments outlined in Table 1. Peak friction varies between experiments based on the effective normal stress and compaction duration.
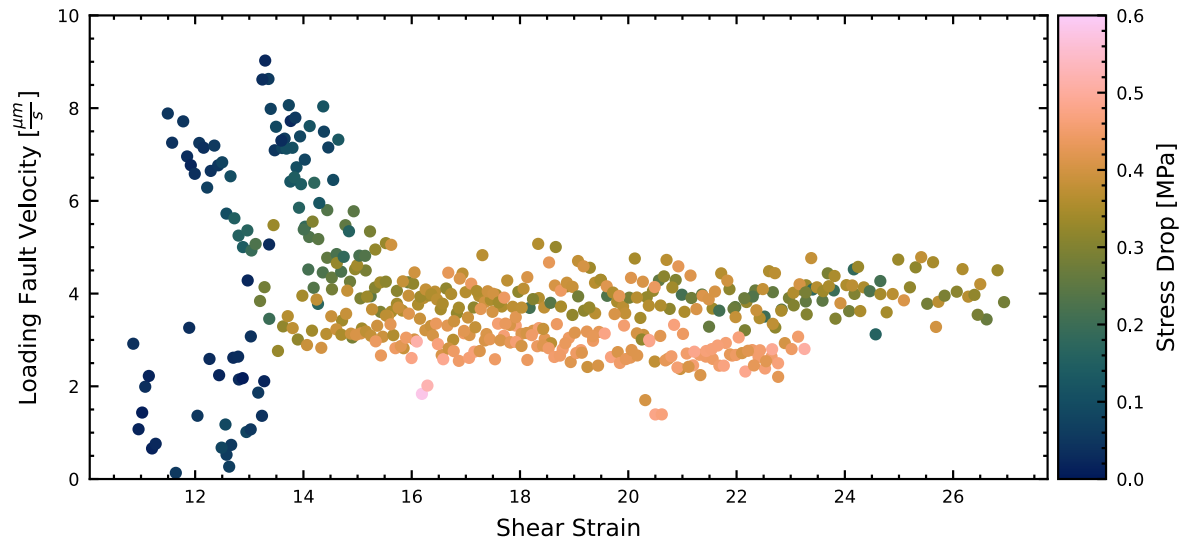
Figure S6. The loading fault creep velocity as a function of shear strain for all experiments. Fault loading creep velocities are measured using the minimum fault velocity during loading. Slower events correspond to low shear strains and stress drops of creep velocities near the background loading rate. Events that have higher shear strain and have greater stress drops are more locked.

March 14, 2023, 9:05pm
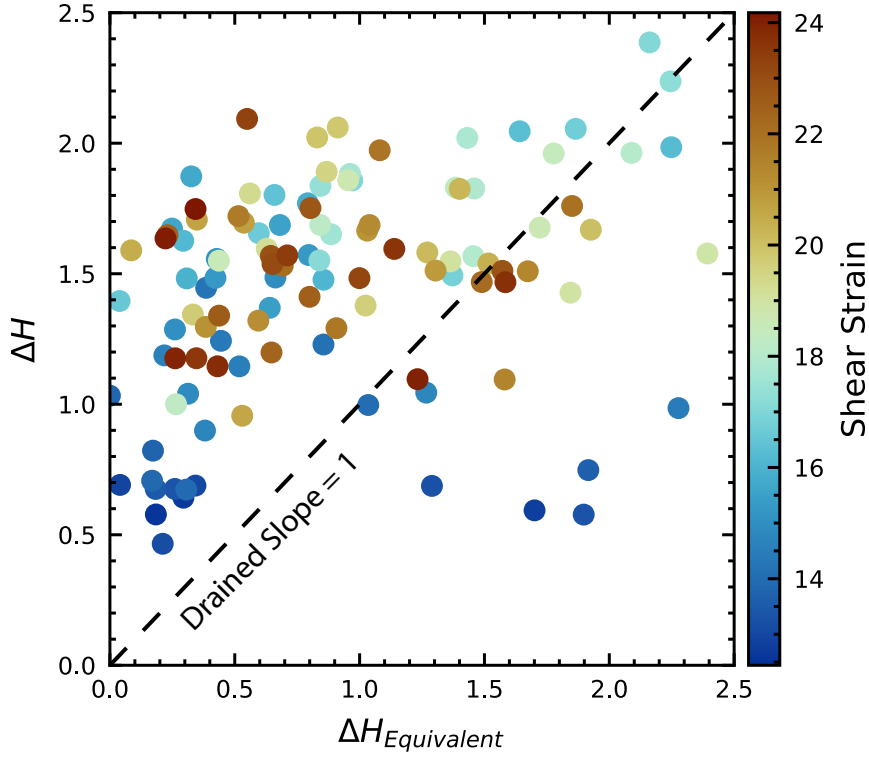
Figure S7. Measured changes in layer thickness (dilation corresponds to positive values of ΔH) vs. changes in layer thickness derived from pore volume measurements ΔV. The fault normal stress is constant so $\Delta V/V$ represents volume strain due to porosity changes and we determine $\Delta H_{Equivlaent}$ from volume strain. When the fault is fully drained these measurements should be equal and have a slope of 1. Our results indicate that the fault behaves predominantly undrained. At high shear strains there is some suggestion of undrained loading but the differences are small and decrease with the magnitude of ΔH, which would indicate drained conditions.

March 14, 2023, 9:05pm
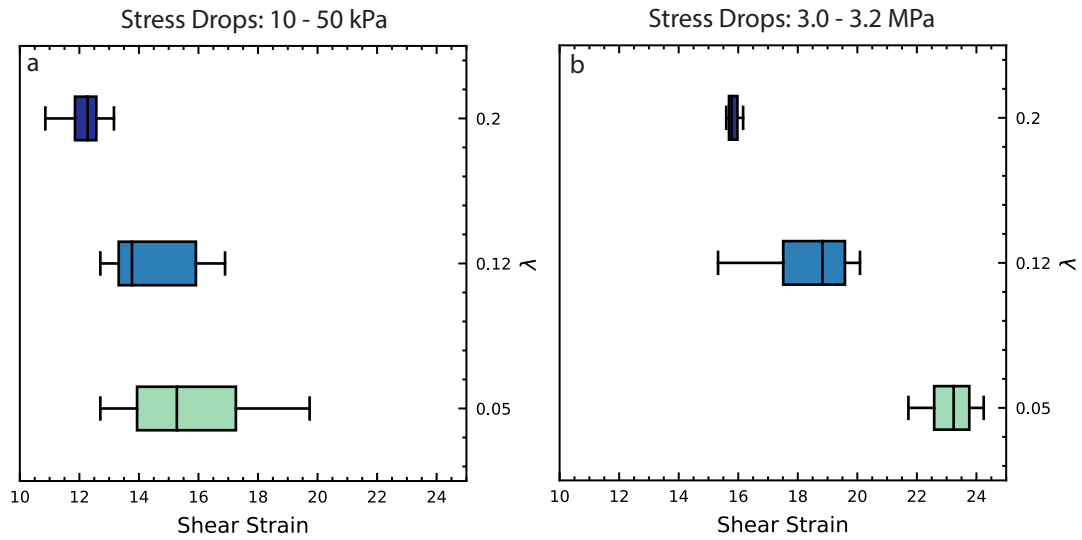
Figure S8. Box and whisker plots for stress drop as a function of strain for all experiments. The distribution of stress drops from 10 - 50kPa shown for each pore pressure condition (a). The distribution of stress drops from 0.3 - 0.32 MPa for each pore pressure condition. The onset of instabilities occurs at lower shear strains for high λ experiments.